



# Fabrication of a porous SiO<sub>2</sub> thin film with an ultralow refractive index for anti-reflective coatings

Ryoko Suzuki <sup>1</sup>

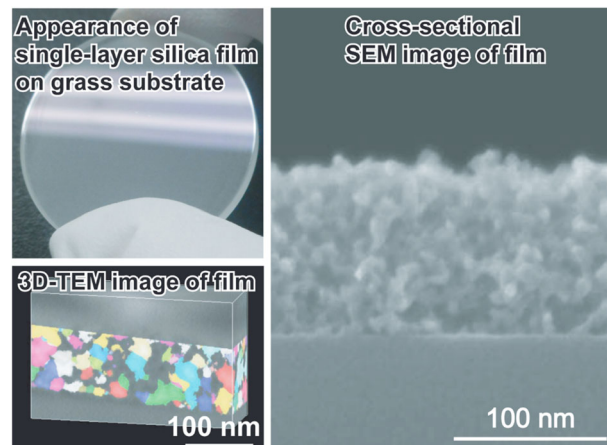
Received: 31 January 2023 / Accepted: 1 April 2023 / Published online: 22 April 2023  
© The Author(s) 2023

## Abstract

Anti-reflective (AR) coatings are used in various optical products, such as lenses, filters, and transparent conductive films. High-performance multilayer AR coatings can be achieved by reducing the refractive index of the top layer. Preventing light scattering by forming finely structured film is also important for a high-performance antireflection film. In this study, porous SiO<sub>2</sub> thin films with ultralow refractive indices were prepared using a simple sol–gel method. A high-quality porous SiO<sub>2</sub> thin film with an ultralow refractive index of 1.17 bearing a fine porous structure was fabricated by carefully selecting the solvent and base species. Observation and simulation of the film structure revealed the factors responsible for the low scattering of light and the ultralow refractive index exhibited by the film. Hydrophobic treatment of the film was conducted to reduce the fluctuation of optical performance caused by changes in the refractive index owing to the water adsorbed. Therefore, porous SiO<sub>2</sub> thin films can be used in the lenses and filters of various optical instruments.

## Graphical abstract

A transparent film with low refractive index was obtained. The film has porous structure, consisting of silica particles of a few nm in size. The pores size was found to be a few nm by image analysis. Thin films with low refractive index and low scattering for optics were successfully prepared by a simple sol–gel method.



**Supplementary information** The online version contains supplementary material available at <https://doi.org/10.1007/s10971-023-06108-8>.

✉ Ryoko Suzuki  
Ryoko.Suzuki@nikon.com

<sup>1</sup> Materials & Research Laboratory, Advanced Technology Research & Development Division, Nikon Corporation, 1-10-1 Asamizodai, Minami-ku, Sagamihara, Kanagawa 252-0328, Japan

**Keywords** Anti-reflective coating · Low refractive index film · Optical thin film · Porous silica

## Highlights

- Ultralow refractive index porous silica film,  $n = 1.17$ , was prepared using a simple sol–gel method.
- Decreasing of light scattering was achieved by choice of basic catalyst and solvent.
- Hydrophobic treatment successfully reduced the fluctuation of the refractive index of the film.

## 1 Introduction

Anti-reflective (AR) coatings are used in various optical products, such as cameras, microscopes, and display panels [1–3]. A multilayer AR coating comprises several stacked layers with varying refractive indices [4]. Among these layers, the top layer contributes the most to AR performance. Decreasing the refractive index ( $n$ ) of the top layer is necessary to improve AR performance.  $\text{MgF}_2$  has the lowest refractive index ( $n = 1.38$ ) but is not sufficiently low for AR coatings [5].

Most low refractive index materials possess a porous structure. The total refractive index of an AR film can be reduced by forming pores containing air ( $n = 1$ ) in the film. To date, various porous materials, such as  $\text{CaF}_2$ ,  $\text{MgF}_2$ , and  $\text{Al}_2\text{O}_3$  have been synthesized [6–8]. In particular,  $\text{SiO}_2$  was focused on materials for preparing porous structures [9–11]. The use of large amount of air to decrease the refractive index of a film tends to cause considerable scattering of light [12, 13]. Moreover, these materials have unstable refractive indices because their pores adsorb moisture from the air easily [14]. To prevent the adsorption of moisture, hydrophilic Si-OH groups of the film surface are often capped. However, the refractive index of the film increases unless the amount of capping agent is controlled [15, 16].

Many studies have reported that a multi-coating of a porous film that contains  $\text{SiO}_2$  and whose refractive index is lesser than 1.20 can achieve high transmittance [17, 18]. Therefore, a thin film with  $n < 1.20$  is required for AR coating. However, porous  $\text{SiO}_2$  thin films prepared via sol–gel reactions often contain large  $\text{SiO}_2$  particles (several tens of nanometers) in their inner structure and exhibit large Rayleigh scattering, which decreases the transmittance of the film [5, 19, 20]. Therefore, a finely structured thin film of porous  $\text{SiO}_2$  is required for optical applications. In this study, an easy sol–gel method was used to prepare porous  $\text{SiO}_2$  thin films. The obtained porous  $\text{SiO}_2$  films exhibited low light scattering and were humidity resistant. In addition, structural analysis and calculations were conducted, and the factors responsible for the low refractive index and scattering were discussed.

## 2 Experiment

### 2.1 Materials

Tetramethyl orthosilicate (TMOS; Tokyo Chemical Industry Co., Ltd.) was used as the silica source. 1-Methoxy-2-propanol (PGME; FUJIFILM Wako Pure Chemical Corporation) was used as a solvent. Triethylamine (TEA; Tokyo Chemical Industry Co., Ltd.) was used as the catalyst for the sol–gel reaction. Hexamethyldisilazane (HMDS; Tokyo Chemical Industry Co., Ltd.) was used for the surface treatment of the porous  $\text{SiO}_2$  thin films.

### 2.2 Sample preparation

The typical preparation methods are described in this section. First, PGME (54.43 g) was poured into a polytetrafluoroethylene (PTFE) bottle.  $\text{H}_2\text{O}$  (1.731  $\mu\text{L}$ ), TEA (36.10  $\mu\text{L}$ ), and TMOS (7.310 g) were then added into the bottle at a molar ratio of TMOS:  $\text{H}_2\text{O}$ : TEA = 1: 2: 0.01 and stirred for ~27 h at the room temperature. The as-prepared coating liquid containing 4.54 wt% of  $\text{SiO}_2$  was filtered using a PTFE filter having a pore size of 5.0  $\mu\text{m}$  and then spin-coated onto a substrate. The films thus obtained were heated to 160 °C for 3 h to obtain a film denoted as  $\text{SiO}_2$ \_PGME\_TEA. After heating, the  $\text{SiO}_2$ \_PGME\_TEA was treated with HMDS to enhance its hydrophobicity. Subsequently, the film, which was coated on a substrate with 30 mm diameter, was sealed in a closed vessel with HMDS (0.6135  $\mu\text{L}$ ) for 24 h at room temperature. Finally, the product was heated at 60 °C for 0.5 h to form  $\text{SiO}_2$ \_HMDS.

### 2.3 Calculation of the refractive index

This research is aimed at obtaining low refractive index thin films. Therefore, the reliability of the refractive index calculation method is very important. The refractive index was calculated with  $\text{SiO}_2$ \_PGME\_TEA described in Experimental procedure. To calculate the refractive index of a thin film with a low refractive index from its reflectance, a substrate with a high refractive index must be used. This is because the greater the difference between the square of the

refractive index of the film and the refractive index of the substrate, the greater the change in reflectance in response to minute changes in the film refractive index, and more reliable the calculation of the refractive index (Eq. (1)) [21].

$$R = \left( (n_s - n^2) / (n_s + n^2) \right)^2 \quad (1)$$

$R$ : reflectance;  $n$ : refract index of thin film;  $n_s$ : refract index of substrate

Therefore, J-SF13 with  $n = 1.74$  (HIKARI GLASS Co., Ltd.), which has the highest refractive index among easily available substrates, was used as the substrate. First, the absence of absorption (extinction coefficient;  $k = 0$ ) in the visible wavelengths (350–800 nm) of SiO<sub>2</sub>\_PGME\_TEA was confirmed via ellipsometry. Reflectance measurements at 350–800 nm deposited on J-SF13 substrates were calculated via fitting with Cauchy's dispersion formula. As a result, the refractive index dispersion shown in Supplementary Fig. S1 was obtained. The refractive index of SiO<sub>2</sub>\_PGME\_TEA was  $n = 1.17$  at 550 nm. Furthermore, reflectance of SiO<sub>2</sub>\_PGME\_TEA on quartz with  $n_d = 1.52$  (HIKARI GLASS Co., Ltd.) and J-BK7A with  $n_d = 1.52$  (HIKARI GLASS Co., Ltd.) showed the same refractive index at 550 nm in case of J-SF13 substrate. The refractive index of SiO<sub>2</sub>\_PGME\_TEA prepared under the reference conditions was reliably determined as  $n = 1.17$ .

The refractive indices of the films prepared by other conditions other than the reference conditions were calculated in the same way as the fitting of refractive index using multiple substrates.

## 2.4 Analysis equipment

Reflectance and transmittance were measured using a UV–vis spectrophotometer (U-3900; Hitachi High-Tech Science Corporation). Refractive indices at 550 nm were calculated using reflectance and TFCalc (HULINKS, Inc.). The intensity of light scattered from the porous SiO<sub>2</sub> thin films coated on quartz substrates was measured using self-assembled equipment composed of an integrating sphere photometer and a light source and was calculated as the sum of intensities of forward- and back-scattered light. The thin films were observed using a scanning electron microscope (SEM, SU9000, Hitachi High-Tech Corporation) and a three-dimensional transmission electron microscope (3D-TEM, JEM-F200, JEOL Ltd.). The pore distribution in the films was analyzed using positron annihilation spectroscopy (PALS-200A, Fuji Imvac Inc.). The contact angles were measured using a contact angle meter (Drop Master DM-501, Kyowa Interface Science Co., Ltd.). Infrared reflection–absorption spectroscopy (IR-RAS) was performed using a spectrometer (FT/IR-6100, JASCO Corporation) with a Vee MAX III variable angle specular reflectance accessory (PIKE

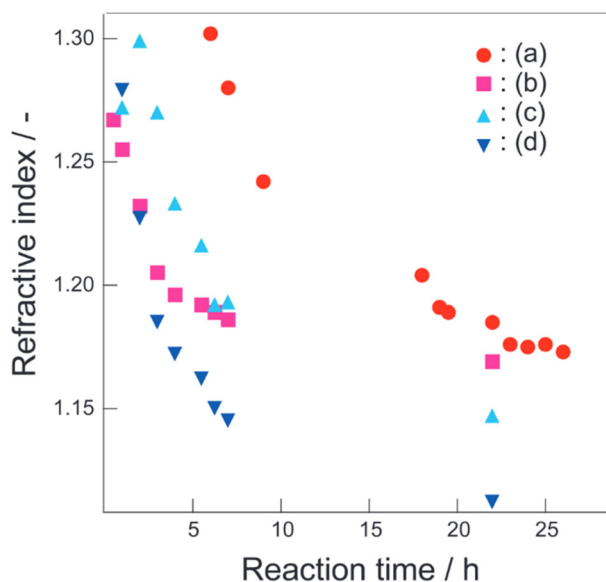


**Fig. 1** Relationship between the sol–gel reaction time and the refractive index of thin films prepared with (a) PGME, (b) methanol, (c) 1-propanol, and (d) 1-pentanol as solvents

Technologies). The packing density of nanoparticles was simulated using Structure of NAno Particles (SNAP) simulation by simulation program SNAP-L ver.3.0.0 (Products Innovation Association).

## 3 Results and discussions

### 3.1 Effect of solvent on SiO<sub>2</sub> thin films

The relationship between the sol–gel reaction time and the refractive index of the films was investigated. In addition, the experiment was repeated with different solvents namely, PGME, methanol, 1-propanol, and 1-pentanol, to investigate the effect of a solvent on the relationship. Figure 1 shows the relationship between the sol–gel reaction time and the refractive index of the prepared films. In all cases, the refractive index decreased with reaction time. This behavior was consistent with previously reported results [22]. The behavior is attributed to generating a bulky structure that consists of SiO<sub>2</sub> and enlarges over time in the reaction mixture. The bulkier the SiO<sub>2</sub> structure, the more the number of and larger pores, formed that contain air. Therefore, the refractive index of the thin films decreases over time. The largest decrease in the refractive index was observed when 1-pentanol was used as a solvent. The refractive indices of the thin films prepared using methanol and 1-propanol were almost equal ( $n \sim 1.20$ ).

Figure 2 shows the relationship between refractive index of the film prepared from the coating liquid reacted for an

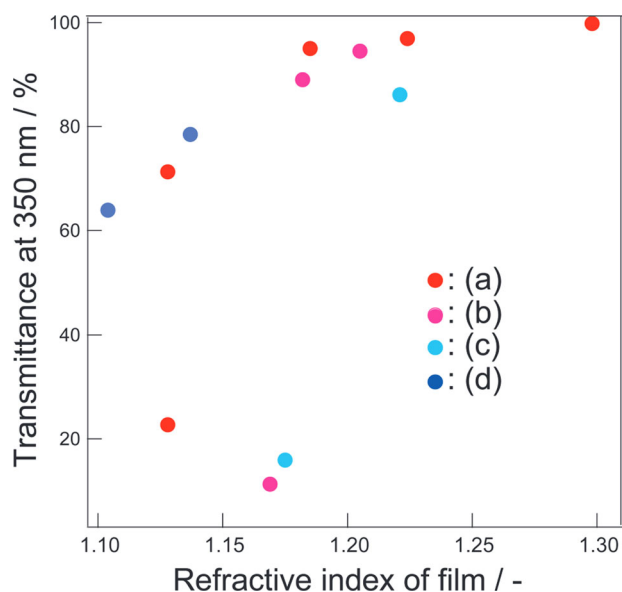


**Fig. 2** Relationship between refraction index of the thin film and the corresponding transmittance at 350 nm of the same coating liquid prepared using (a) PGME, (b) methanol, (c) 1-propanol, and (d) 1-pentanol

arbitrary time and transmittance at 350 nm of the same coating liquid for different solvents. In all cases, the transmittance and refractive index decreased with reaction time simultaneously. As shown in Fig. 1, SiO<sub>2</sub> structures grew and aggregated in coating liquid during the sol–gel reaction, which increased the porosity of the SiO<sub>2</sub> thin films. Figure 2 provides data to consider how SiO<sub>2</sub> fine structure can be formed without particle growth and aggregation, increasing scattering and decreases transmittance. The transmittance corresponding to PGME was higher than that corresponding to methanol and 1-propanol when the refractive indices of the thin films were almost the same; for example, the refractive index was approximately 1.20. The reaction mixture containing 1-pentanol exhibits the highest transmittance. These results indicate that finely structured SiO<sub>2</sub> was formed when PGME and 1-pentanol were used as solvents.

The results showed transesterification occurred between the methoxy group of TMOS and the solvent during the sol–gel reaction. The reactivity of silanes that underwent transesterification was lower than that of TMOS, possibly because silanes contain a bulkier alkoxy group than TMOS. The bulky alkoxy group on the surface of the SiO<sub>2</sub> structure prevented the aggregation of the SiO<sub>2</sub> particles. The transesterification reaction also prevented the growth and aggregation of SiO<sub>2</sub> structures. In addition, PGME is considered a suitable solvent for controlling the refractive index of AR coatings because it tends to reduce the refractive index near 1.20 gradually.

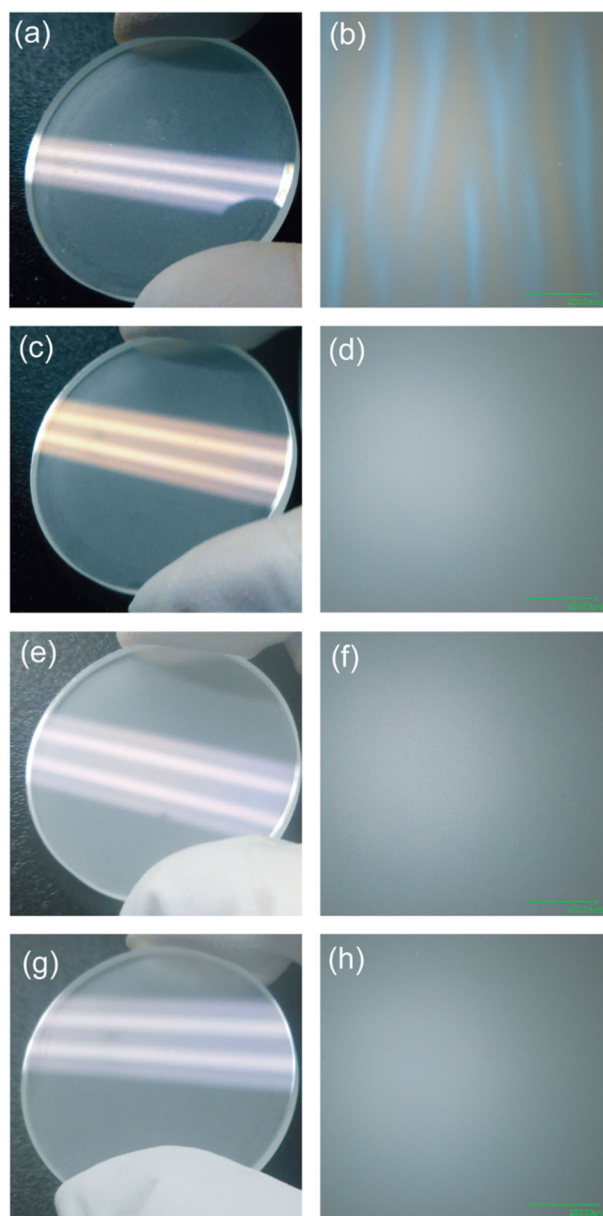
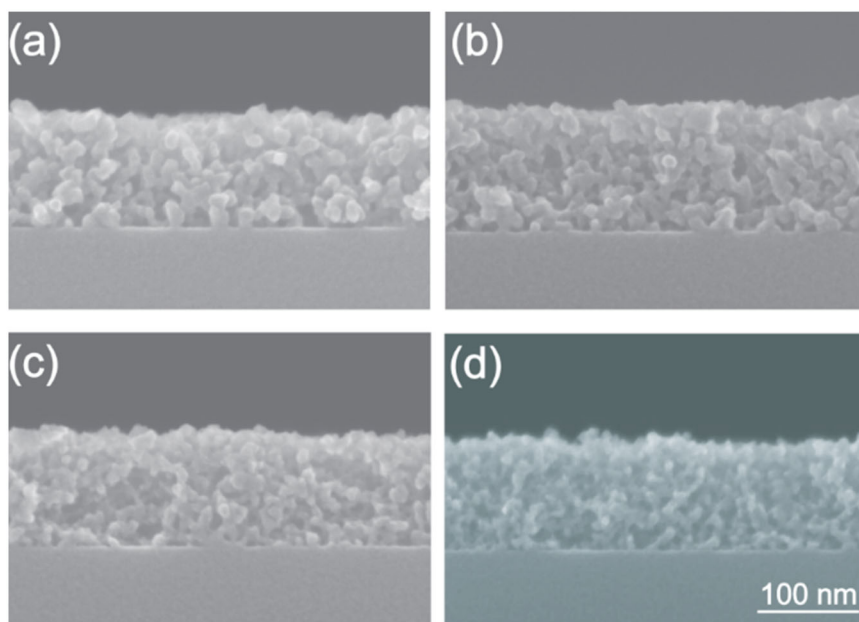


**Fig. 3** Appearance of a thin film prepared using a coating liquid containing (a) methanol, (c) 1-propanol, (e) 1-pentanol, and (g) PGME; b, d, f, and h represent the corresponding optical microscopic images

Figure 3 shows the photographs and optical microscopic images of the thin films prepared in this study. As shown in Fig. 3a, b, radial striations can be observed in the SiO<sub>2</sub> thin film surface prepared using methanol. In contrast, thin films prepared using 1-propanol (Fig. 3c, d), 1-pentanol (Fig. 3e, f), and PGME (Fig. 3g, h) exhibit smooth surfaces.

From the above results, PGME can be considered a suitable solvent for fabricating porous silica thin films as AR coating from view points of control of refractive index and appearance.

**Fig. 4** Cross-sectional SEM images of (a) SiO<sub>2</sub>\_PGME\_NH<sub>3</sub>, (b) SiO<sub>2</sub>\_PGME\_PA, (c) SiO<sub>2</sub>\_PGME\_DEA, and (d) SiO<sub>2</sub>\_PGME\_TEA



### 3.2 Effect of the base on the structure of porous SiO<sub>2</sub> thin films

To investigate the effect of the base on the structure of SiO<sub>2</sub> thin films, SiO<sub>2</sub> thin films were prepared using NH<sub>3</sub>, propylamine (PA), and diethylamino (DEA) in place of TEA in the original preparation method. In each experiment, the refractive index of the thin films was adjusted to  $n = 1.17$  by controlling the reaction time.

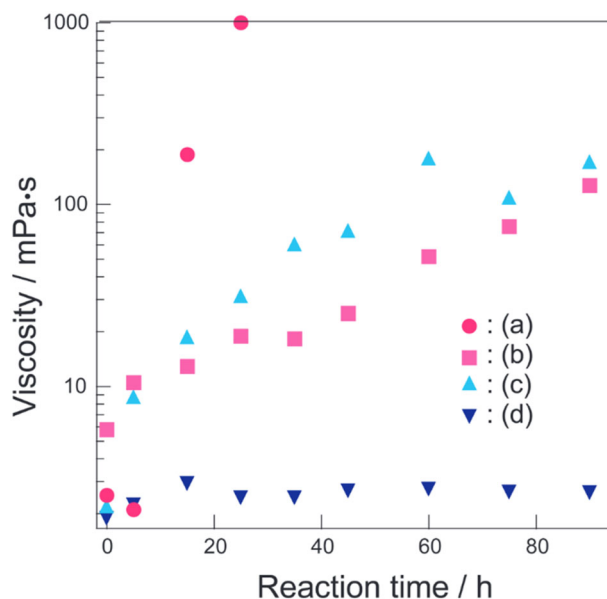
Figure 4 shows the cross-sectional SEM images of the thin films. A SiO<sub>2</sub> framework comprising small connected particles was observed in all porous SiO<sub>2</sub> thin films. In Fig. 4, the diameter of a SiO<sub>2</sub> primary particle was considered corresponding to the thickness of the framework. Therefore, the SiO<sub>2</sub> primary particle diameter was measured at four points and averaged in each SEM image (Fig. S2). SiO<sub>2</sub>\_PGME\_NH<sub>3</sub> (Fig. 4a) and SiO<sub>2</sub>\_PGME\_PA (Fig. 4b) possessed thick frameworks. The second thinnest and thinnest frameworks were observed in SiO<sub>2</sub>\_PGME\_DEA (Fig. 4c) and SiO<sub>2</sub>\_PGME\_TEA (Fig. 4d), respectively. The thicknesses of the SiO<sub>2</sub>\_PGME\_NH<sub>3</sub>, SiO<sub>2</sub>\_PGME\_PA, SiO<sub>2</sub>\_PGME\_DEA, and SiO<sub>2</sub>\_PGME\_TEA frameworks, measured using their SEM images, were 15.8, 15.3, 11.0, and 9.8 nm, respectively.

Table 1 shows the amount of scattered light at 350 nm by thin films. The amount of light scattered by SiO<sub>2</sub>\_PGME\_PA was the highest, whereas that scattered by SiO<sub>2</sub>\_PGME\_TEA was the smallest.

Figure 5 shows the viscosity of the reaction mixture to reaction time. The viscosity increased with reaction time for samples prepared using PA, DEA, and TEA catalysts. Notably, the maximum increase in viscosity is observed for

**Table 1** Amount of scattered light at 350 nm by the porous SiO<sub>2</sub> thin films

Sample	Amount of scattering at 350 nm/ppm
SiO <sub>2</sub> _PGME_NH <sub>3</sub>	248
SiO <sub>2</sub> _PGME_PA	388
SiO <sub>2</sub> _PGME_DEA	265
SiO <sub>2</sub> _PGME_TEA	204



**Fig. 5** Viscosity of the reaction mixture containing (a) TEA, (b) DEA, (c) PA, and (d) NH<sub>3</sub> as the catalyst to reaction time

TEA. The type of basic catalyst affected the formation of  $\text{SiO}_2$  because of the inductive effect, steric hindrance of the catalysts and solvent [23]. The pKa values of  $\text{NH}_3$ , propylamine, diethylamine and triethylamine in water are 9.21, 10.53, 10.98 and 10.65, respectively [24]. It means that basicity decreases in the order diethylamine > triethylamine > propylamine >  $\text{NH}_3$ . However, the pKa values listed here are those in water, which have been widely reported, and these values vary with the solvent. It has been reported that tertiary amines may have a higher pKa than secondary amines in organic solvents [25]. This is owing to the stability of the generated cationic species in the solvent and other factors. Therefore, it must be noted that the reaction of this study was carried out in an organic solvent, mainly PGME. Furthermore, the composition of solvent was changed with the progress of reaction owing to methanol produced by hydrolysis. Therefore, discussing the reactivity of the base from the pKa value of a particular solvent is difficult. However, TEA has the highest reactivity in PGME than other bases. This may be because TEA has three alkyl chains, which are electron-donating groups, and the  $\text{NH}(\text{C}_2\text{H}_5)_3^+$  generated from TEA has stability in organic solvents owing to its three alkyl chains. SEM images and viscosity measurements showed that small  $\text{SiO}_2$  nanoparticles were simultaneously generated and interconnected when TEA was used as a basic catalyst.

These results indicate that the structure of the porous  $\text{SiO}_2$  thin films differed depending on the organic base used. In particular, a fine-structured low-scattering film was obtained using a highly basic catalyst (TEA). However, gelation did not proceed when  $\text{NH}_3$  was used as a basic

catalyst. The refractive index of the thin film could be decreased by interlinking small  $\text{SiO}_2$  nanoparticles using TEA and by growing  $\text{SiO}_2$  nanoparticles using  $\text{NH}_3$ . In conclusion, TEA is a suitable catalyst for synthesizing porous  $\text{SiO}_2$  thin films for AR coating.

### 3.3 Inner and surface structure of a thin film

The Structural characteristics of  $\text{SiO}_2$ \_PGME\_TEA ( $n = 1.17$ ) were investigated. Figure 6 shows the pore distribution measured via positron annihilation spectroscopy. Two peaks were observed at 0.48 nm and 2.4 nm. The peak at 0.48 nm could be attributed to the gap in the siloxane framework [26] and that at 2.4 nm could be ascribed to the presence of pores in  $\text{SiO}_2$  films.

Figure 7 shows a 3D-TEM image of  $\text{SiO}_2$ \_PGME\_TEA. The colored areas represent pores that were detected by image analysis. Several pores were distributed inside the film. Image analysis also revealed the pore distribution (Supplementary Fig. S3), which showed that the pore diameter was in the range of 2–3 nm. This is consistent with the results induced via positron annihilation spectroscopy. Additionally, porosity was calculated to be 65 vol % via image analysis. Considering that the refractive index calculated from the reflectance measurement was  $n = 1.17$ , the porosity of the film was calculated from the Lorentz–Lorentz formula using the refractive index of  $\text{SiO}_2$  and air and their volume fractions [27]. The porosity calculated using the refractive index was 62.2 vol %. This result indicates that a 3D-TEM structural analysis was appropriate. Therefore,  $\text{SiO}_2$ \_PGME\_TEA was confirmed to possess abundant pores of diameter 2–3 nm and a high porosity of over 60 vol%. This high porosity was attributed to the bulky colloidal  $\text{SiO}_2$  structure grown in the coating liquid. If  $\text{SiO}_2$  in the coating liquid were mono-dispersed spherical particles, the porosity of porous  $\text{SiO}_2$  thin films would be 49.4 vol%, as calculated using SNAP simulation (Supplementary Fig. S4) [28, 29]. This shows that the  $\text{SiO}_2$  in the

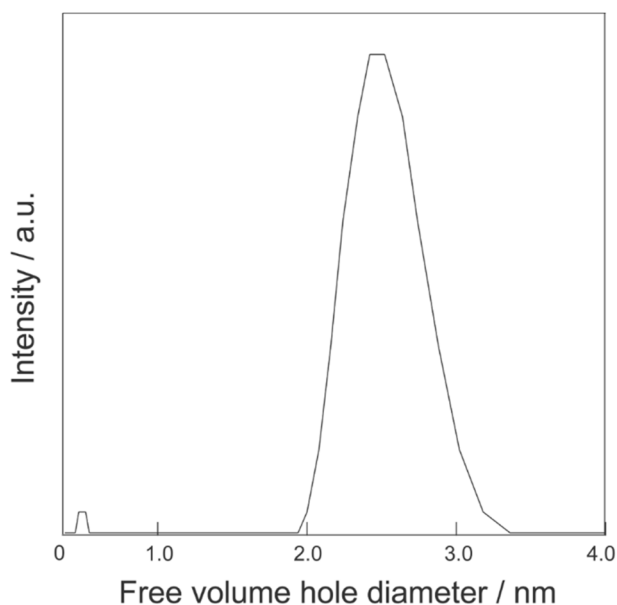


**Fig. 6** Pore size distribution of  $\text{SiO}_2$ \_PGME\_TEA ( $n = 1.17$ ) measured using positron annihilation spectroscopy

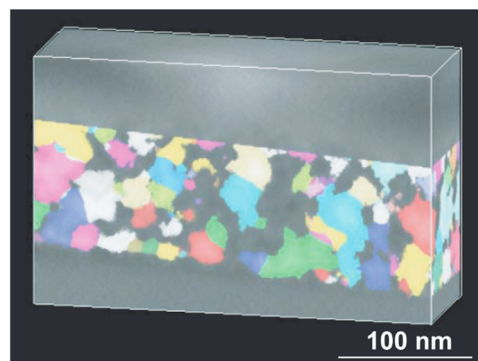


**Fig. 7** 3D-TEM image of  $\text{SiO}_2$ \_PGME\_TEA. The refractive indices of the films were adjusted to  $n = 1.17$ . Colored areas were detected pores using image analysis

coating liquid possessed a bulky structure formed by connecting small SiO<sub>2</sub> nanoparticles. Because bulky SiO<sub>2</sub> structures could not be densely packed like mono-dispersed spherical nanoparticles, they formed a highly porous SiO<sub>2</sub> thin film.

The size of the pores in SiO<sub>2</sub>\_PGME\_TEA (2–3 nm) was smaller than the wavelength of visible light, indicating that SiO<sub>2</sub>\_PGME\_TEA can exhibit a low scattering of light [30].

### 3.4 Enhanced hydrophobicity of SiO<sub>2</sub>\_PGME\_TEA

The adsorption of moisture from air into porous SiO<sub>2</sub> was reported to increase the refractive index [14]. When porous SiO<sub>2</sub> is used for AR coating, increasing the refractive index

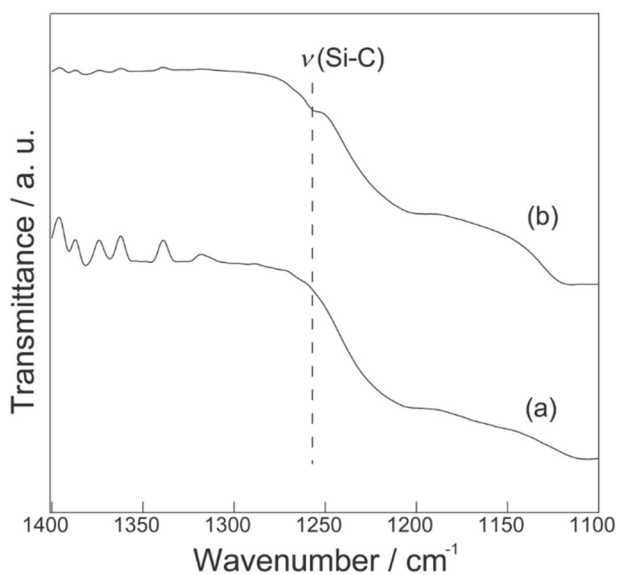


**Fig. 8** RAS-IR spectra of SiO<sub>2</sub>\_PGME\_TEA (a) before and (b) after HMDS treatment

**Fig. 9** Contact angle measurement of SiO<sub>2</sub>\_PGME\_TEA (a) before and (b) after HMDS treatment

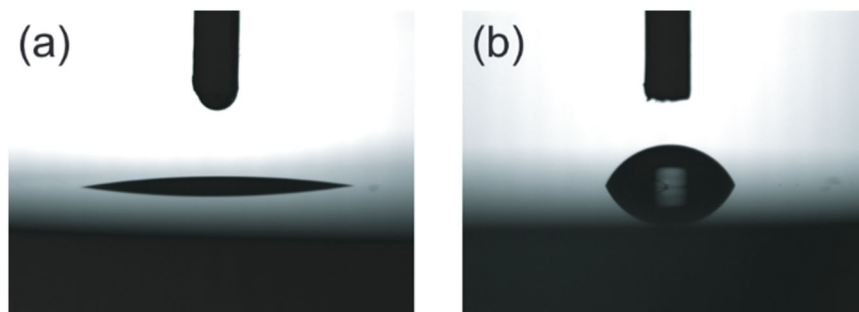


**Table 2** Refractive indices of SiO<sub>2</sub>\_PGME\_TEA and SiO<sub>2</sub>\_HMDS on 0, 1, and 7 d

	<i>n</i> on day 0	<i>n</i> on day 1	<i>n</i> on day 7	Increase in <i>n</i> after 1 d	Increase in <i>n</i> after 7 d
SiO <sub>2</sub> _PGME_TEA	1.170	1.198	1.212	0.028	0.014
SiO <sub>2</sub> _HMDS	1.197	1.201	1.209	0.004	0.008

affects the optical properties. Therefore, the Si–OH groups in SiO<sub>2</sub>\_PGME\_TEA should be capped by hydrophobic groups. HMDS was used for capping the Si–OH groups because it is commonly used for hydrophobization [31].

Figure 8 shows the IR-RAS spectra of SiO<sub>2</sub>\_PGME\_TEA and SiO<sub>2</sub>\_HMDS. An adsorption band at 1250 cm<sup>−1</sup> was observed in SiO<sub>2</sub>\_HMDS spectra, which was assigned to  $\nu$  (Si–C) [32]. It showed that HMDS was introduced into SiO<sub>2</sub>\_PGME\_TEA.

In addition, the contact angles of SiO<sub>2</sub>\_PGME\_TEA and SiO<sub>2</sub>\_HMDS were measured to be 8.7° and 65°, respectively (Fig. 9). This indicated that SiO<sub>2</sub>\_PGME\_TEA possessed a hydrophilic surface, whereas SiO<sub>2</sub>\_HMDS possessed a hydrophobic surface. These results revealed that HMDS successfully capped the Si–OH group and increased the hydrophobicity of SiO<sub>2</sub>\_PGME\_TEA.

The refractive indices of SiO<sub>2</sub>\_PGME\_TEA and SiO<sub>2</sub>\_HMDS are listed in Table 2. The refractive index of SiO<sub>2</sub>\_HMDS was higher than that of SiO<sub>2</sub>\_PGME\_TEA. It probably indicated that HMDS was introduced into the pores of SiO<sub>2</sub>\_PGME\_TEA. Moreover, the changes in refractive indices after keeping the films at 24 °C and 35% relative humidity for 1 d and 7 d were compared. The increase in the refractive index of SiO<sub>2</sub>\_HMDS was smaller than that of SiO<sub>2</sub>\_PGME\_TEA for both 1 and 7 d.

Hence, the HMDS treatment prevented an increase in the refractive index of the porous SiO<sub>2</sub> thin films via the capping of the Si–OH groups.

## 4 Conclusion

Porous SiO<sub>2</sub> thin films having low refractive indices were successfully prepared via a simple sol–gel method. The choice of solvent and basic catalyst is a key factor for controlling the reactivity of the coating liquid and

forming a smooth film that exhibits low scattering. The porous SiO<sub>2</sub> thin film fabricated in this study could be used as a broadband AR coating with stacked under-coating and as a lens and sensor in various optical devices.

**Acknowledgements** The author wishes to acknowledge Mr. Masahiro Ousaka (Nikon Corp.) for the valuable simulation using SNAP, a part of optical measurement and optical simulations.

**Author contributions** RS contributed to all the study's conception and design. RS performed material preparation and data collection. RS wrote the manuscript.

## Compliance with ethical standards

**Conflict of interest** The author declares no competing interests.

**Publisher's note** Springer Nature remains neutral with regard to jurisdictional claims in published maps and institutional affiliations.

**Open Access** This article is licensed under a Creative Commons Attribution 4.0 International License, which permits use, sharing, adaptation, distribution and reproduction in any medium or format, as long as you give appropriate credit to the original author(s) and the source, provide a link to the Creative Commons license, and indicate if changes were made. The images or other third party material in this article are included in the article's Creative Commons license, unless indicated otherwise in a credit line to the material. If material is not included in the article's Creative Commons license and your intended use is not permitted by statutory regulation or exceeds the permitted use, you will need to obtain permission directly from the copyright holder. To view a copy of this license, visit <http://creativecommons.org/licenses/by/4.0/>.

## References

- Shanbhogue HG, Nagendra CL, Annapurna MN, Kumar SA, Thutupalli GKM (1997) Multilayer antireflection coatings for the visible and near-infrared regions. *Appl Opt* 36:6339–6351
- Li X, Gao J, Xue L, Han Y (2010) Porous polymer films with gradient-refractive-index structure for broadband and omnidirectional antireflection coatings. *Adv Funct Mater* 20:259–265
- Chen D (2001) Anti-reflection (AR) coatings made by sol-gel processes: A review. *Solar Sol Energy Mater Sol Cells* 68:313–336
- Sun X, Tu J, Li L, Zhang W, Hu K (2020) Preparation of wide-angle and abrasion-resistant multi-layer antireflective coatings by MgF<sub>2</sub> and SiO<sub>2</sub> mixed sol. *Colloids Surf A* 602:125106
- Zhang X, Lan P, Lu Y, Li J, Xu H, Zhang J, Lee YP, Rhee JY, Choy KL, Song W (2014) Multifunctional antireflection coatings based on novel hollow silica-silica nanocomposites. *ACS Appl Mater Interfaces* 6:1415–1423
- Thomas IM (1988) Porous fluoride antireflective coatings. *Appl Opt* 27:3356–3358
- Fujihara S, Kadota Y, Kimura T (2002) Role of organic additives in the sol-gel synthesis of porous CaF<sub>2</sub> anti-reflective coatings. *J Sol Gel Sci Tech* 24:147–154
- Yamaguchi N, Tadanaga K, Matsuda A, Minami T, Tatsumisago M (2007) Antireflective properties of flowerlike alumina thin films on soda-lime silica glass substrates prepared by the sol-gel method with hot water treatment. *Thin Solid Films* 515:3914–3917
- Thomas IM (1986) High laser damage threshold porous silica antireflective coating. *Appl Opt* 25:1481–1483
- Moghal J, Kobler J, Sauer J, Best J, Gardener M, Watt AAR, Wakefield G (2012) High-performance, single-layer antireflective optical coatings comprising mesoporous silica nanoparticles. *ACS Appl Mater Interfaces* 4:854–859
- Vincent A, Babu S, Brinley E, Karakoti A, Deshpande S, Seal S (2007) Role of catalyst on refractive index tunability of porous silica antireflective coatings by sol-gel technique. *J Phys Chem C* 111:8291–8298
- Peeters MPJ, Bohmer MR (2003) Optical application of (pigmented) sol-gel coatings. *J Sol Gel Sci Technol* 26:57–62
- Murray C, Flannery C, Streiter I, Schulz SE, Baklanov MR, Mogilnikov KP, Himcinschi C, Friedrich M, Zahn DRT, Gessner T (2002) Comparison of techniques to characterise the density, porosity and elastic modulus of porous low-k SiO<sub>2</sub> xerogel films. *Microelectron Eng* 60:133–141
- Wang Z, Gu Z (2009) Optical humidity-sensitive mechanism based on refractive index variation. *Chin Opt Lett* 7:756–759
- Dou W, Wang P, Zhang D, Yu J (2016) An efficient way to prepare hydrophobic antireflective SiO<sub>2</sub> film by sol-gel method. *Mater Lett* 167:69–72
- Zhang S, Xiao P, Wang P, Luo J, Jiang B (2020) Spherical-chain silica with super-hydrophobic surface and ultra-low refractive index for multi-functional broadband antireflective coatings. *Sol Energy* 207:1222–1230
- Huang X, Yuan Y, Liu S, Zhang L, Hong R (2018) Preparation of hydrophobic broadband antireflective SiO<sub>2</sub> coating on flexible poly (methyl methacrylate) substrates. *Colloid Surf A Physicochem Eng Asp* 538:519–525
- Hsu H-T, Ting C-Y, Mou C-Y, Wan B-Z (2003) Nanoporous SiO<sub>2</sub> films prepared by surfactant templating method - a novel antireflective coating technology. *Stud Surf Sci Catal* 146:539–542
- Ren H, Zhu J, Bi Y, Xu Y, Zhang L (2018) Assembly of methylated hollow silica nanospheres toward humidity-resistant antireflective porous films with ultralow refractive indices. *J Porous Mater* 25:55–62
- Rouse JH, Ferguson GS (2003) Preparation of thin silica films with controlled thickness and tunable refractive index. *J Am Chem Soc* 125:15529–15536
- Rand MJ (1970) Spectrophotometric thickness measurement for very thin SiO<sub>2</sub> films on Si. *J Appl Phys* 41:787
- Makita K, Akamatsu Y, Takamatsu A (1999) Sol-gel preparation of silica films with controlled surface morphology and their application to a low reflective glass. *J Sol Gel Sci Technol* 14:175–186
- Hancock RD, Nakani BS, Marsicano F (1983) Relationship between Lewis acid-base behavior in the gas phase and in aqueous solution. I. Role of inductive, polarizability, and steric effects in amine ligands. *Inorg Chem* 22:2531–2535
- Coetzee JF, Padmanabhan GR (1965) Properties of bases in acetonitrile as solvent. IV. Proton acceptor power and homo-conjugation of mono- and diamines. *J Am Chem Soc* 87:5005–5010
- Cantu MD, Hillebranda S, Carrilho E (2005) Determination of the dissociation constants (pK<sub>a</sub>) of secondary and tertiary amines in organic media by capillary electrophoresis and their role in the electrophoretic mobility order inversion. *J Chromatogr A* 1068:99–105
- Misheva M, Djourellov N, Margaca FMA, Salvado IMM (2001) Positronium study of porous structure of sol-gel prepared SiO<sub>2</sub>: influence of pH. *J Non Cryst Solids* 279:196–203



27. Falcaro P, Grosso D, Amenitsch H, Innocenzi P (2004) Silica orthorhombic mesostructured films with low refractive index and high thermal stability. *J Phys Chem B* 108:10942–10948
28. Hasegawa K, Nasu A, Fuita M (2016) Behavior analysis of coating layer particles in cosmetic materials during drying by observation and computational simulation. *Josai Math Monogr* 9:75–88
29. Fujita M, Yamaguchi Y (2006) Development of three-dimensional structure formation simulator of colloidal nanoparticles during drying. *J Chem Eng Jpn* 39:83–89
30. Jain PK, Lee KS, El-Sayed IH, El-Sayed MA (2006) Calculated absorption and scattering properties of gold nanoparticles of different size, shape, and composition: applications in biological imaging and biomedicine. *J Phys Chem B* 110:7238–7248
31. Nalamasu O, Cheng M, Timko AG, Pol V, Reichmanis E, Thompson LF (1991) An overview of resist processing for deep-UV lithography. *J Photopolym Sci Technol* 4:299–318
32. Hirotsu T, Tagaki C (2004) Plasma copolymer membranes of acrylic acid and the adsorption of lysozyme on the surface. *Thin Solid Films* 457:20–25